Experimental Detection and Quantification of Structural Nonlinearity Using Homogeneity and Hilbert Transform Methods

Kragh, Knud Abildgaard; Thomsen, Jon Juel; Tcherniak, Dmitri

Published in:
Proceedings of ISMA2010-USD2010

Publication date:
2010

Document Version
Publisher's PDF, also known as Version of record

Experimental Detection and Quantification of Structural Nonlinearity Using Homogeneity and Hilbert Transform Methods

K. A. Kragh [1], **J. J. Thomsen** [2], **D. Tcherniak** [3]
[1] Technical University of Denmark, Risø National Laboratory for Sustainable Energy,
Frederiksborgvej 399, P.O. Box 49 , Building 118, 4000 Roskilde, Denmark
e-mail: **knkr@risoe.dtu.dk**

[2] Technical University of Denmark, Department of Mechanical Engineering,
Nils Koppels Alle, Building 404, 2800 Lyngby, Denmark

[3] Brüel & Kjær Sound and Vibration Measurement,
Skodsborgvej 307, 2850 Nærum, Denmark

Abstract
All real structures are inherently nonlinear. Whether a structure exhibits linear or nonlinear behavior, depends mainly on the excitation level. So far no unequivocal framework for experimental detection, localization, and characterization of structural nonlinearities from dynamic measurements exists. The present study suggests a framework for the detection of structural nonlinearities. Two methods for detection are compared, the homogeneity method and a Hilbert transform based method. Based on these two methods, a nonlinearity index is suggested. Through simulations and laboratory experiments it is demonstrated, for a simple but representative nonlinear structure, that both detection methods are able to detect even weak nonlinearities, and that the nonlinearity index provides a sensitive and robust measure of nonlinearity. For a range of input force amplitudes, it is shown that it is possible to estimate a systems linear and nonlinear regimes in terms of input amplitude, and asses the strength of the nonlinearity.

1 Introduction

Systems are often referred to as being linear or nonlinear. However, all system are inherently nonlinear, though for many systems it is possible to linearize around an operating point. If energy is pumped into a system with increasing intensity, the system will at some point start behaving nonlinearly, e.g. the system might break or collide with other systems. In essence a system behaving nonlinearly is a system where the response is not linearly related to the input. Hence a linear system is a convenient mathematical abstraction. Linear systems holds many convenient features: Linear systems have only one equilibrium position, the principle of super position is valid, and many linear models are more or less alike and described by well proven theories. Nonlinear systems typically have multiple equilibria, both stable and unstable, the principle of super position is not valid, the system might exhibit chaotic motions, and exact analytic solutions are only available for a few special cases.

Tools for detection, quantification, localization and characterization of nonlinearities in engineering structures from experimental observations would be useful in a number of applications, e.g.:

- *Model validation and improvement* Methods for detecting and quantifying nonlinearities could help validating linear models and establishing ranges of validity of linear models. With a known range of

validity it should be possible to determine whether to use a linear or nonlinear model. Furthermore, identified nonlinearities can be implemented in nonlinear models, thus improving the models.

- *Structural health monitoring* Many types of structural damage and malfunctions will manifest them self as structural nonlinearities. One example of this is breathing cracks, which is essentially a bilinear stiffness nonlinearity. Reliable methods for detection, quantification and localization of nonlinearities from operational measurements could reduce inspection times and enable technicians to detect damage otherwise not visible on the structure.

- *Sensor fault detection* Accelerometers and other dynamic transducers are widely used in industry to measure and monitor the dynamics of structures. The measurements are only reliable when the sensors are working properly. A malfunctioning sensor, e.g. a sensor that is partly detached from the structure will typically act as a structural nonlinearity. Detection and localization methods could enable users to pinpoint the defect sensor.

The first prerequisite for such applications is the ability to detect structural nonlinearities experimentally from dynamic measurements, which is the focus of this present study.

In [1] a survey of the most common methods for identification of structural nonlinearities is given. Other suggested methods include [2] and [3] in which spectral densities are used for detection, [4] suggests a detection method based on reciprocal modal vectors, [5] suggests a pattern recognition method, [6] and [7] describe how the Hilbert transform can be used for detection, and [8] and [9] uses the concept of nonlinear normal modes for detection and characterization of nonlinearity.

For this present study the Hilbert transform based method and the homogeneity method are selected. Mainly because of their practical applicability, but also because they allow a way of quantifying the nonlinearity by introducing a nonlinearity index. The two methods will first be tested on a simulation model, to gain knowledge of the performance in a noise free environment. The methods are then applied to an experimental system to gain knowledge of the methods performance in a more realistic setting.

First the homogeneity method, Hilbert transform based method, and nonlinearity index are introduced, then modeling and results from both simulated and experimental study are provided, and finally discussed.

2 Methods for Detection and Quantification

2.1 The Homogeneity Method

The simplest approach for the detection of structural nonlinearity is based on exploiting that the frequency response function (FRF) of linear systems is independent of input amplitude. In the following this feature is referred to as the *homogeneity* of a system [1]. In contrast to linear systems, the FRF of a nonlinear system depends on the input force magnitude. E.g. a system with a hardening cubic nonlinearity will exhibit an increase of the resonant frequencies with increasing input force.

A large challenge when using the homogeneity condition for detection is quantifying the FRF distortion and providing a measure of the nonlinearity level with physical meaning. In the literature there seems to be no unequivocal way of doing this. Here we present a suggestion based on cross correlating FRFs. Conventionally the cross correlation $R_{ab}(\tau)$ of two functions $a(t)$ and $b(t)$ in time domain is defined as:

$$R_{ab}(\tau) = \int_{-\infty}^{\infty} a(t)b(t+\tau)dt \tag{1}$$

In the present application, the cross correlation is used in the frequency domain with two FRFs, $H^H(\omega)$ and $H^L(\omega)$:

$$R_{H^H H^L}(\Delta\omega) = \int_{-\infty}^{\infty} H^H(\omega) H^L(\omega + \Delta\omega) d\omega \tag{2}$$

where $H^H(\omega)$ and $H^L(\omega)$ are FRFs obtained with high and low level excitation, respectively. The cross correlation is a measure of how closely correlated the two FRFs are as a function of a frequency shift $\Delta\omega$. Using the normalized cross correlation a value, $R_{H^1 H^2}(\Delta\tilde{\omega}) = 1$ implies that the two FRFs are identical at lag $= \Delta\tilde{\omega}$. The cross correlation is normalized such that the auto correlations are unity at $\Delta\omega = 0$.The squared normalized correlation coefficient is a measure of how much of the variance in the two functions that is shared. Using the cross correlation with the FRFs of a given system excited at two input levels, provides information on how the FRF is distorted in the applied input range. If the squared cross correlation of the two FRFs is 1 at a lag of 0 Hz, then there is no FRF distortion in the applied input range due to nonlinearity. If there is no FRF distortion, the system behaves linearly in the input range. Since the FRF distortion is a direct indication of nonlinearity, the squared cross correlation coefficient at lag $\Delta\omega = 0$ will be used as a quantitative measure of the strength of the nonlinearity in the applied input range. The value of $\Delta\omega$ giving the highest correlation coefficient is an estimate of the shift of resonance frequency in the input amplitude range. The squared normalized cross correlation coefficient will in the following be referred to as the nonlinearity index δ_{Ho}:.

$$\delta_{Ho} = ||R_{H^H H^L}(0)||^2 \tag{3}$$

where $||R_{H^H H^L}||$ is the normalized cross correlation coefficient, H^L is the FRF of the system excited at a low level, and H^H is the FRF of the system excited at a high level.

Note that δ_{Ho} will only indicate if the system is behaving linearly or nonlinearly in the applied input amplitude range. Also, since the nonlinearity index is based on cross correlating FRFs, the index will have high sensitivity to nonlinearities shifting the resonant frequency, and less sensitivity to nonlinearities, which only scales the FRF magnitude.

2.1.1 Steps of the Homogeneity Method

1. Excite the system at two input levels within the operating range of the structure and measure the response.
2. Calculate the FRFs from low level and high level excitation. The low and high level excitation should reflect the operating range of the structure. The Low level excitation should be sufficiently high, so that the coherence of averaged FRFs is close to unity in the applied frequency range. The high level excitation should reflect the highest operating level of the system.
3. Calculate and evaluate the cross correlation of the two FRFs
   (a) If the nonlinearity measure δ_{Ho} exhibits values below unity, then the system exhibits nonlinearity in the applied excitation range.
   (b) The shift of resonant frequency can be estimated as the value of $\Delta\omega$ giving the highest cross correlation coefficient.

2.2 The Hilbert Transform Based Method

The Hilbert transform is an integral transform, as the Fourier transform. In contrast to the Fourier transform, the Hilbert transform maps functions into the same domain.The Hilbert transform $\mathscr{H}$ of a FRF $H(\omega)$ is defined in [6] as:

$$\mathscr{H}(H(\omega)) = \frac{1}{i\pi} PV \int_{-\infty}^{\infty} \frac{H(\omega)}{\Omega - \omega} d\Omega \tag{4}$$

where PV denotes the Cauchy principal value of the integral, which is needed since the integrand has a singularity. The Cauchy principal value is used to estimate the value of improper integrals, so that for any function $f(x)$ with a singularity at $x = b$:

$$PV \int_a^c f(x)dx \equiv \lim_{\epsilon \to 0^+} \left[\int_a^{b-\epsilon} f(x)dx + \int_{b+\epsilon}^c f(x)dx \right] \tag{5}$$

If the Hilbert transform is applied to a FRF, $G(\omega)$, of a linear system, the transform will relate the imaginary part of the FRF to the real part [6]:

$$Re(G(\omega)) = -\frac{1}{\pi} PV \int_{-\infty}^{\infty} \frac{Im(G(\omega))}{\Omega - \omega} d\Omega \tag{6}$$

$$Im(G(\omega)) = \frac{1}{\pi} PV \int_{-\infty}^{\infty} \frac{Re(G(\omega))}{\Omega - \omega} d\Omega \tag{7}$$

Hence the Hilbert transform of the FRF of a linear system will return the original FRF, the real part of the transformed FRF is the imaginary part of the original FRF and vice versa. Equation (6) and (7) are referred to as the Hilbert transform pairs. For nonlinear systems (6) - (7) is not generally valid, hence the Hilbert transform of the FRF of a nonlinear system will return a distorted version of the FRF. The distortion, hence the level of nonlinearity is quantified in a similar manner as for the homogeneity method, using the squared cross correlation coefficient:

$$\delta_{Hi} = ||R_{\mathcal{H}H}(0)||^2 \tag{8}$$

where $||R_{\mathscr{H}H}||$ is the normalized cross correlation coefficient, H is the FRF of the system and $\mathscr{H}$ is the Hilbert transform of H, and:

$$R_{\mathcal{H}H}(\Delta\omega) = \int_{-\infty}^{\infty} \mathcal{H}(\omega) H(\omega + \Delta\omega) d\omega \tag{9}$$

Note that δ_{Hi} will only indicate if the system is behaving linearly or nonlinearly at the applied input amplitude.

2.2.1 Steps of the Hilbert Transform based Method

1. Excite the structure at an input level in the upper range of the the operating range of the structure, and measure the response.
2. Calculate the FRF, H, and its Hilbert transform $\mathcal{H}$.
3. Calculate the nonlinearity index δ_{Hi}
   (a) If $\delta_{Hi} < 1$, then the system exhibits nonlinearity at the applied excitation amplitude.

2.3 The Methods Compared

The homogeneity methods has the advantage of providing a physical measure of the change in system behavior in a given input range, δ_{Ho} will indicate how the system behaves in a certain amplitude range. On the other hand, the homogeneity method requires two series of excitation, whereas the Hilbert transform based method only requires one.

3 Benchmark Model

To test and compare the performance of the methods, a mechanical benchmark model was used. This model constitutes the raw concept of what was realized in the laboratory, and simplified in a numerical model.

The N dof lumped mass model, cf. Figure 1, is essentially linear and was chosen because it is simple and resembles a variety of structures of engineering interest. Nonlinearities, $Q_i(x_i, \dot{x}_i)$, of different types can be added to the underlying linear system and tested. The implementation of the nonlinearities in the simulation and experimental model, respectively, is given in the section 4 and 5. The mathematical model of the benchmark model is:

$$\mathbf{M}\ddot{\mathbf{x}} + \mathbf{C}\dot{\mathbf{x}} + \mathbf{K}\mathbf{x} + \mathbf{q}(x, \dot{x}) = \mathbf{f} \tag{10}$$

where $\mathbf{M}$ is the mass matrix, $\mathbf{C}$ the damping matrix, $\mathbf{K}$ the stiffness matrix, $\mathbf{q}(x, \dot{x})$ a vector containing nonlinear terms, $\mathbf{f} = \mathbf{f}(t)$ the forcing vector and $\mathbf{x} = \mathbf{x}(t) \in R$ the deflection vector.

4 Simulation Study

4.1 Simulation model

To evaluate the detection methods, a simulation model based on Equation (10) is implemented. Excitation of the model is constant amplitude swept sines. Three types of nonlinearities are implemented: cubic stiffness (ϵx_i^3), cubic damping ($\epsilon \dot{x}_i^3$), and a nonsmooth stiffness nonlinearity (ϵx_i), where ϵx_i is defined as:

$$\epsilon = 0, \quad x_i < x_{stop} \tag{11}$$

$$\epsilon = 10^3 \cdot k_i, \quad x_i \leq x_{stop} \tag{12}$$

All simulations are carried out with the parameters given in Table 1 using MATLAB's ODE45 solver.

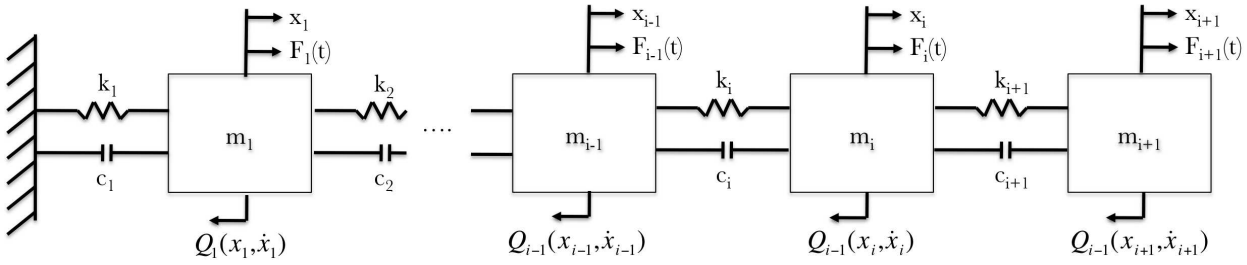

Figure 1: Mechanical model, where m_i is mass of dof i, k_i and c_i is the linear stiffness and damping connecting the dof's in the model, x_i is the displacement of the i'th dof, $f_i(t)$ is the applied force acting on dof i, $Q_i(x, \dot{x})$ is a grounded nonlinearity acting on dof i, and N is the number of dofs in the system.

Table 1: Parameters for simulations

Sampling frequency	500 Hz
Input sweep range	0 to 50 Hz
Sweep rate	0.5 Hz/s
Discrete masses m_i	1 Kg
Linear stiffness k_i	1500 N/m
Damping coefficient c_i	1
FRF estimator	H1

To compare the performance of the two methods, a frame of reference is introduced. Both methods are tested at different levels of nonlinearity. Therefore a measure of the nonlinearity level is needed. Equation (10) can be multiplied by $\dot{\mathbf{x}}^T$ and terms expressing the instantaneous power of the linear stiffness/damping forces and the total power of the nonlinear forces can be identified:

$$\dot{\mathbf{x}}^T\mathbf{M}\ddot{\mathbf{x}} + \overbrace{\dot{\mathbf{x}}^T\mathbf{C}\dot{\mathbf{x}}}^{P_{lin,damp}} + \overbrace{\dot{\mathbf{x}}^T\mathbf{K}\dot{\mathbf{x}}}^{P_{lin,stiff}} + \overbrace{\dot{\mathbf{x}}^T\mathbf{q}(x,\dot{x})}^{P_{nonlin}} = \dot{\mathbf{x}}^T\mathbf{f} \tag{13}$$

In the following the *level of nonlinearity* in the systems being simulated, is defined as the fraction of the root mean square (RMS) over time of the power terms:

$$\eta = \frac{RMS(P_{nonlin\{damp/stiff\}})}{RMS(P_{lin\{damp/stiff\}})} \tag{14}$$

where

$$RMS(P_{nonlin/lin\{damp/stiff\}}) = \sqrt{\frac{1}{t_{end}-t_{start}}\int_{t_{start}}^{t_{end}} P_{nonlin/lin\{damp/stiff\}}dt} \tag{15}$$

The results of the simulations with smooth nonlinearities will be evaluated using η. The results for the nonsmooth nonlinearities will be plotted as a function of the maximum displacement of the dof associated with the nonlinearity.

4.2 Simulation Results

Only results for a 3-dof system are presented. Systems with up to 9 dofs were tested, but the results from the 3-dof case are representative for all the tested cases. The methods are tested on the same data sets, and the results are therefore directly comparable.

4.2.1 The Homogeneity Method

Figure 2 shows results obtained with the Homogeneity method applied to a system with a cubic stiffness nonlinearity. It is evident that δ_{Ho} diverges from unity at approximately $\eta > 10^{-2.5}$. Hence the nonlinearity is detected at this magnitude of nonlinearity.

Figure 3 shows the results obtained with the Homogeneity method applied to a system with a nonsmooth nonlinearity. A very clear limit between the system's linear and nonlinear regime is apparent. When the displacement amplitude does not exceed the position of the stop, then $\delta_{Ho} = 1$. When the stop is hit, δ_{Ho} decreases radically. The lowest values of δ_{Ho} are found when using the FRF based on the output gathered at the dof associated with the nonlinearity.

Figure 4 shows results obtained with the Homogeneity method applied to a system with a cubic damping nonlinearity. It appears that the decrease of δ_{Ho} from unity occurs at a much higher value of η compared to the case with the smooth stiffness nonlinearity. This is because the resonance peak is not shifted as with the stiffness nonlinearity case. Since the FRF is not shifted but only lowered in magnitude, the cross correlation coefficient will not decrease as much as in the stiffness nonlinearity case.

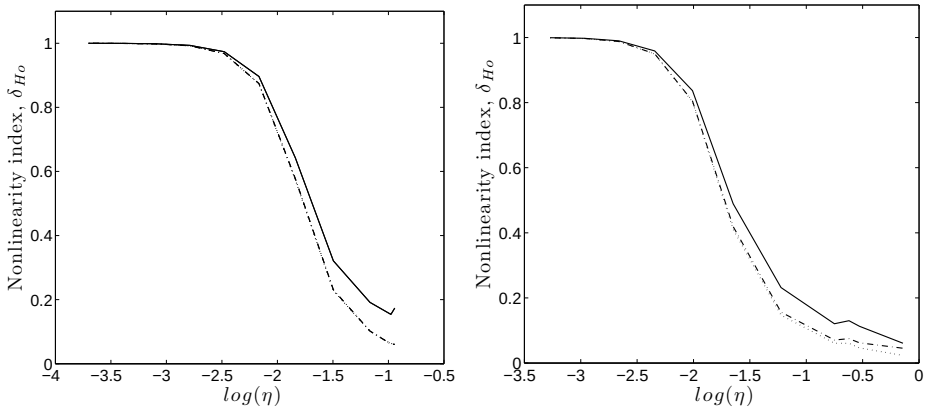

(a) (b)

Figure 2: Nonlinearity index δ_{Ho} as a function of nonlinearity level η. Simulation results with the homogeneity method applied to a 3-dof system with fixed input levels of 1 and 50 N and increasing magnitude of cubic nonlinearity ϵ_i, at position: (a) dof 2 (b) dof 3. The nonlinearity index is calculated based on all possible FRFs: H_{11} $(-)$, H_{12} $(\cdots)$, and H_{13} $(- \cdot -)$

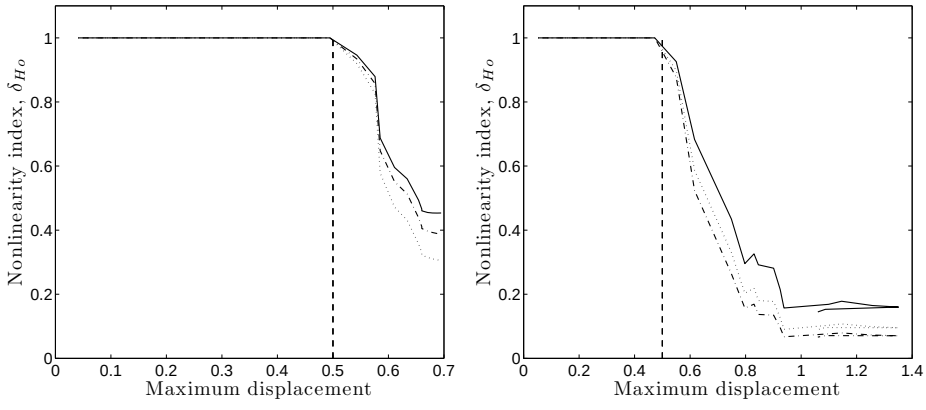

(a) (b)

Figure 3: Nonlinearity index δ_{Ho} as a function of the maximum displacement of the dof associated with the nonlinearity. Simulation results from the homogeneity method applied to a 3 dof system with hard stop at $x_i = 0.5$ and increasing input force. (a) Gap at dof 2, (b) Gap at dof 3. The nonlinearity index is calculated based on all three possible FRF's: : H_{11} $(-)$, H_{12} $(\cdots)$, and H_{13} $(- \cdot -)$. $(--)$ indicates position of hard stop

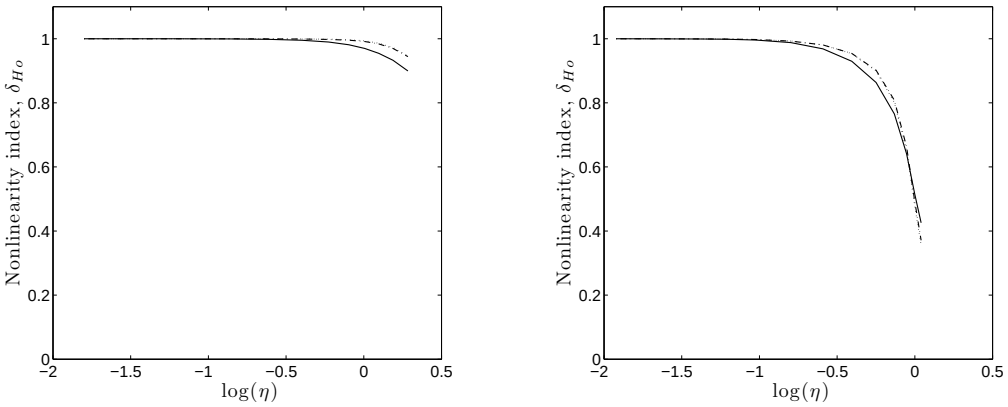

(a) (b)

Figure 4: Nonlinearity index δ_{Ho} as a function of nonlinearity level η. Simulation results from the homogeneity method applied to a 3 dof system with an increasing cubic damping nonlinearity. (a) Nonlinearity at dof 1, (b) Nonlinearity at dof 3. Swept sine excitation with amplitude 1 and 50 Newtons at dof 1. The nonlinearity index is calculated based on all three possible FRF's: H_{11} $(-)$, H_{12} $(\cdots)$, and H_{13} $(-\cdot-)$

4.2.2 Hilbert Transform Based Method

Figure 5 shows the results from the system with a cubic stiffness nonlinearity and Figure 6 with a nonsmooth stiffness nonlinearity. From Figure 5 it is seen that the drop in δ_{Hi} occurs at approximately $\eta = 10^{-1}$. This is a larger value than the one obtained using the homogeneity method, hence the Hilbert transform method is not as sensitive as the homogeneity method. It is also noted that the drop in δ_{Hi} is not as distinct as for the homogeneity method. Figure 6 shows a drop of δ_{Hi} when the deflection amplitude of the dof associated with the nonlinearity reaches $x_i = 0.5$, but the drop is far from as distinct as for the homogeneity method. For the case with the nonlinearity associated with dof 2, the drop is hardly significant.

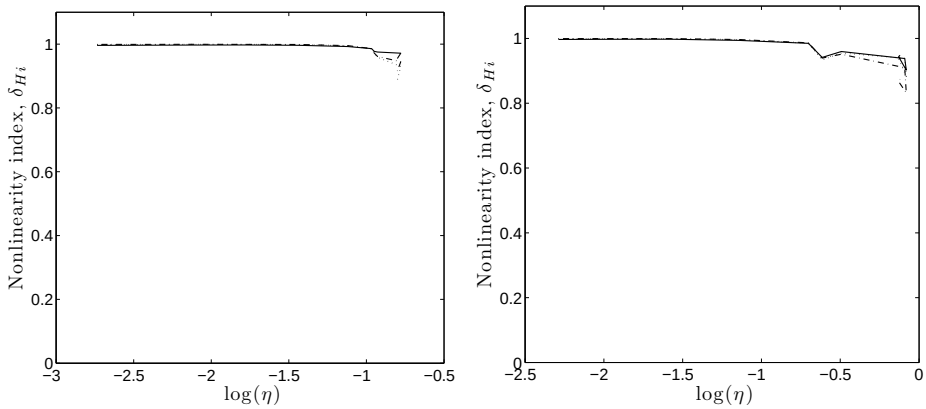

(a) (b)

Figure 5: Nonlinearity index of Hilbert transform based method applied to a 3-dof system with increasing coefficient of cubic stiffness nonlinearity, ϵ_i as a function of nonlinearity level η. Simulation perform with constant force and increasing coefficient of cubic term. (a) Nonlinearity at dof 2, (b) Nonlinearity at dof 3. H_{11} $(-)$, H_{12} $(\cdots)$, and H_{13} $(-\cdot-)$

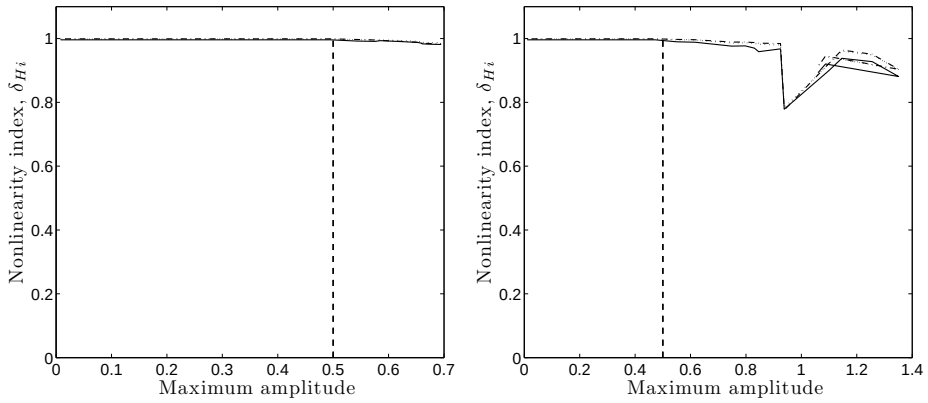

(a) (b)

Figure 6: Nonlinearity index of Hilbert transform based method applied to a 3-dof system with gap nonlinearity placed at $x_i = 0.5m$. Simulations performed with increasing force. (a) Nonlinearity at dof 2, (b) Nonlinearity at dof 3.H_{11} $(-)$, H_{12} $(\cdots)$, and H_{13} $(- \cdot -)$. Position of hard stop $(--)$

5 Experimental Testing

To asses the practical capabilities of the detection methods, the methods were applied to experimental data.

5.1 Experimental model

The experimental setup is shown in Figure 7. The accelerations are measured at each of the three masses attached to the clamped beam, and a vibration shaker provides force at dof 1. This setup is chosen because the behavior of the system in the frequency range covering the lowest three modes can be described by 13

In the simulated study a linear swept sine excitation was used, but due hardware limitations an exponential sweep is used in the experimental case. Parameters for the experiment are given in Table 2, and the equipment used is listed in Table 3.

In the experimental tests the same types of stiffness nonlinearities as in the simulation study will be realized, smooth and nonsmooth. The implementation of these two nonlinearities is shown in Figure 11. The smooth nonlinearity is realized using opposing neodymium magnets whereas the nonsmooth nonlinearity is realized using a one sided mechanical rigid stop with an attached rubber piece to avoid high frequency components induced by the impacts.

If results should be directly comparable to the simulation study, the smooth nonlinearity in the experimental setting should be cubic. This is ensured by testing the static stiffness of the system with and without the smooth nonlinearity attached, using a laser displacement sensor and a dynamometer, see Figure 9(a)

Table 2: Parameters for experimental tests of detection methods

	3 dof system
Excitation type	Exponential sweep
Sweep rate	0.036 decades/sec
Excitation duration	64 sec
Excitation dof	1
Frequency range	0-100 Hz
Frequency lines	6400

Table 3: Equipment

Description	Official name
Accelerometers	B&K: 4507B, 4507, 4508, 4399
Force transducer	Endevco: 2312 + B&K: 2646
Shaker	B&K 4810
Front end	B&K Slots: 3109, 3032A
Software	B& K Pulse
Fixtures	Aluminium
Masses	Aluminium
Beam	Hardened stell 400 x 35 x 1.5 mm

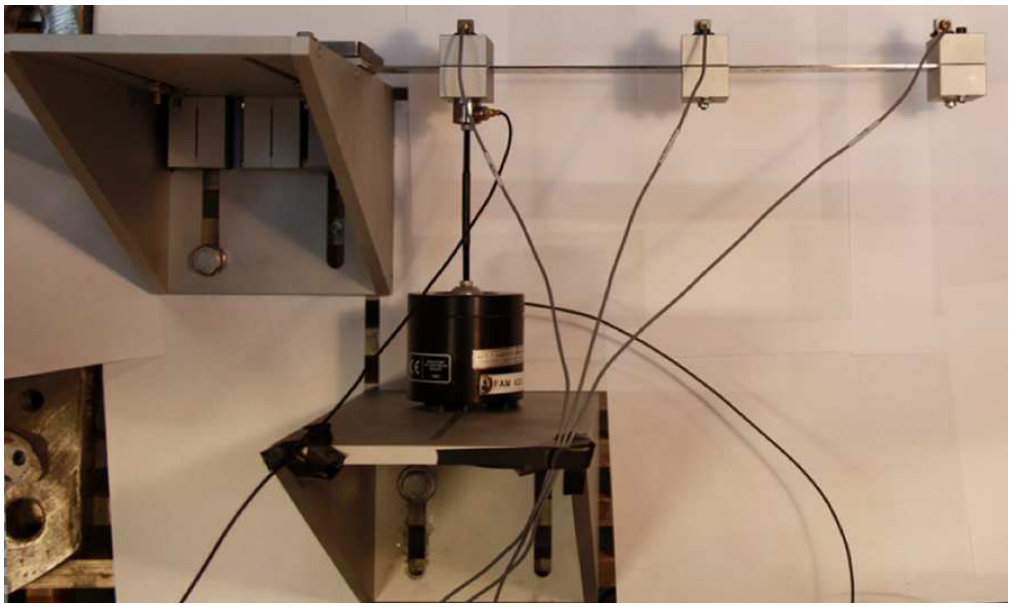

Figure 7: Experimental model, top-view.

From Figure 9(b) it is seen that with no nonlinearities attached, the stiffness is linear in the tested displacement range, whereas with the magnets attached (Figure 9(c)) the stiffness off the system appears to be cubic. The linear domain indicated in Figure 9(c) is defined as the range in which a straight line can be fitted to the data with a correlation coefficient larger that 0.99.

5.2 Experimental Results

5.2.1 Homogeneity Method

Figure 10(a) and 10(b) shows δ_{Ho} as a function of the displacement when the homogeneity method is applied to a 3 dof system with a smooth stiffness nonlinearity at dof 2 and a 3 dof system with a nonsmooth nonlinearity at dof 2, respectively.

With the smooth nonlinearity attached it appears that δ_{Ho} is approximately unity at displacements below 7 mm. At displacements larger than $\approx 7mm$, δ_{Ho} drops, hence indicating nonlinear behavior. This displacement corresponds approximately to the limits of the estimated linear domain defined in Figure 9.

From Figure 10(b) it seen that δ_{Ho} drops when the hard stop is hit ($x_2 = 7mm$), indicating nonlinear behavior at displacements larger than the distance to the stop. The largest drop in δ_{Ho} is seen when δ_{Ho} is

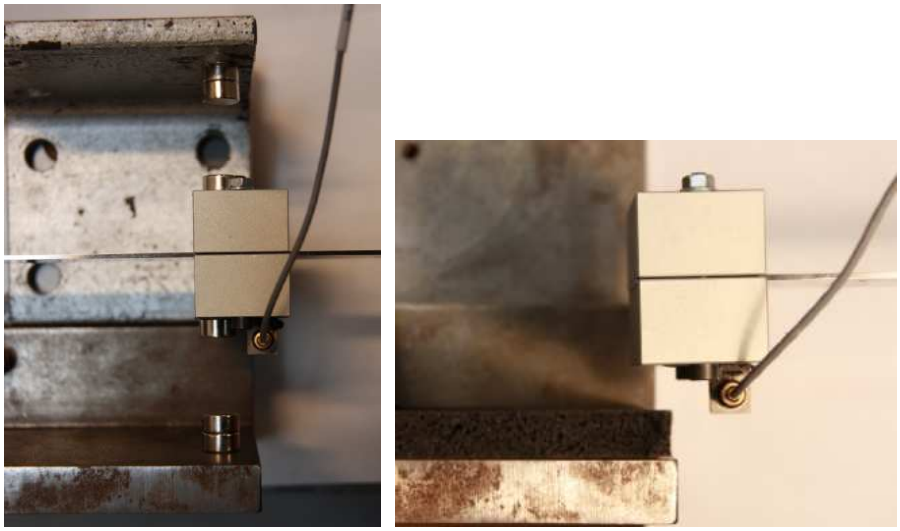

(a) (b)

Figure 8: Realization of nonlinearities: a) Smooth nonlinearity, by opposing magnets, b) nonsmooth nonlinearity, by hard stop with rubber.

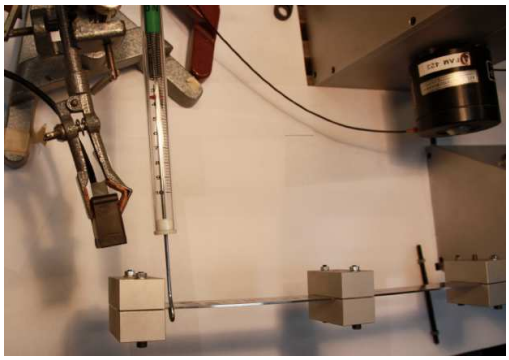

(a)

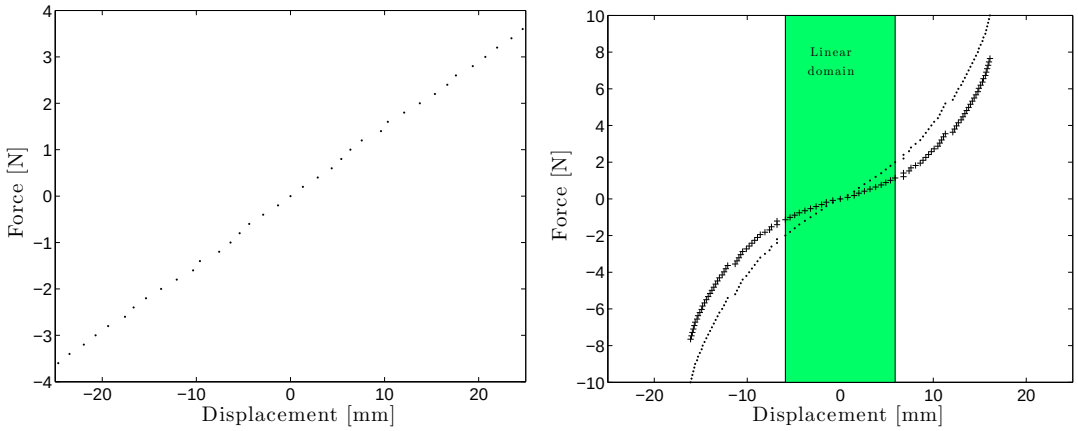

(b) (c)

Figure 9: a) Experimental setup for static test without nonlinearity b) Force measured by dynamometer as a function of displacement from static test without nonlinearity c) Force measured by dynamometer as a function of displacement from static test with smooth nonlinearity attached. Measured values ($\cdot\cdot\cdot$), Measured values, with linear stiffness subtracted ($+++$)

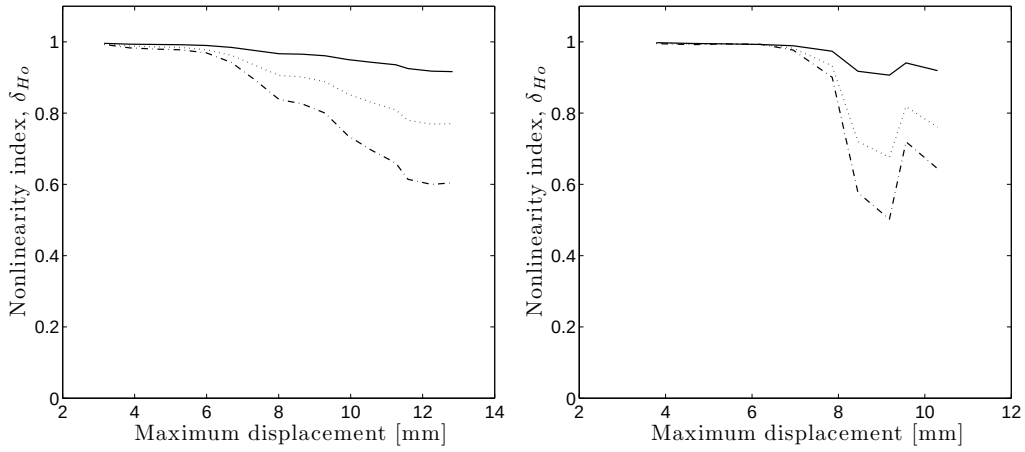

(a) (b)

Figure 10: Nonlinearity index δ_{Ho} as a function of displacement when the homogeneity method applied to a 3 dof system a with: a) A smooth nonlinearity (magnets) at dof 2. Constant low level excitation and increasing high level excitation. Low level amplitude (RMS): 0.80 N. b) A nonsmooth nonlinearity (hard stop). Constant low level excitation and increasing high level excitation. Stop at dof 2 (distance to stop: 7 mm), low level amplitude (RMS): 0.81 N. H_{11} $(-)$, H_{12} $(\cdot\cdot)$, and H_{13} $(-\cdot-)$

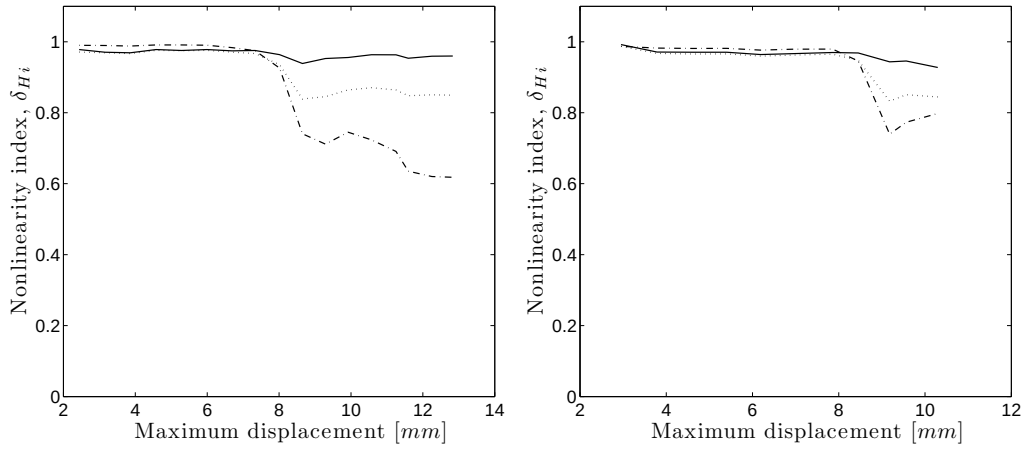

(a) (b)

Figure 11: Nonlinearity index δ_{Hi} as a function of displacement when the homogeneity method applied to a 3 dof system a with: a) A smooth nonlinearity (magnets) at dof 2. Constant low level excitation and increasing high level excitation. Low level amplitude (RMS): 0.80 N. b) A nonsmooth nonlinearity (hard stop). Constant low level excitation and increasing high level excitation. Stop at dof 2 (distance to stop: 7 mm), low level amplitude (RMS): 0.81 N. H_{11} $(-)$, H_{12} $(\cdot\cdot)$, and H_{13} $(-\cdot-)$

calculated from H_{12}, indicating this as the position of the stop. The system was tested with the nonlinearity at the two other position, but there were no consistency in the indications of the location of the nonlinearities.

5.2.2 Hilbert Transform Based Method

Figure 11(a) shows the results from applying the Hilbert transform based method on the 3 dof system with a smooth stiffness nonlinearity at dof 2 are shown. Figure 11(b) shows the result when the Hilbert transform based method is applied to a 3 dof system with a nonsmooth nonlinearity at dof 2.

From figures 11(a) and 11(b) it seen that in both cases the decrease in the detection parameter, δ_{Hi}, occurs at

a larger deflection amplitudes than with the homogeneity method. This corresponds to the results from the simulation study.

6 Discussion

6.1 Homogeneity Method

The homogeneity method gives a measure of the physical change in system behavior, and is easy to relate to, even without much knowledge of nonlinear systems. Since the nonlinearity index is based on cross correlating FRFs at two levels of input, the value of the index is greatly dependent on the range of excitation amplitudes. It is therefore necessary to establish an amplitude range of the system under study before applying the method. The FRFs tested must represent the operating range of the system. The low level excitation must be at the lowest possible level of excitation giving a satisfying coherence. The high level excitation must be at the highest operating level. In this way, nonlinear behavior in the operating range will be captured. As a consequence, conclusions can only be drawn for the excited amplitude range.

Since the nonlinearity index is based on the cross correlation, the method is most sensitive to nonlinearities shifting the resonant frequency. Damping nonlinearities, which only change the height of the resonance peaks, will not result in a drop in the nonlinearity index as distinct as with a stiffness nonlinearity, even at equal levels of nonlinearity. Since the effect of a damping nonlinearity on a system is not as radical as the effect of a stiffness nonlinearity, the less distinct detection might not be an issue. An issue with the nonlinearity index, which is not assessed in this study, is that its sensitivity depends on the width of the resonance peaks, and hence of the damping of the system. If the system is only lightly damped and has very narrow resonance peaks, even small frequency shifts will produce a low nonlinearity index, indicating a strong nonlinearity. To obtain a low index for a highly damped system the frequency shift has to be very large. Again this resembles the actual behavior of the system, and might not be problematic. The phenomena might be overcome by introducing a term in the nonlinearity index, correcting for the observed damping of the system.

6.2 Hilbert Transform Based Method

Since the nonlinearity index obtained from the Hilbert transform based method is based on the cross correlation function, the method suffers from the same problems as the homogeneity method. The Hilbert transform based method requires only excitation at one level for the method to detect a nonlinearity. The excitation must be sufficiently high for the nonlinearity to become significant. It is therefore recommended to apply the method to data obtained at the system's highest operating level. Again conclusions can only be drawn for the system at the excited amplitude. To get a more thorough knowledge of the system, tests should be performed at varying input levels.

6.3 Excitation

In this study the excitation was performed using a sweept sine forcing. Since both methods are based on frequency domain data, the excitation could also have been of other types, e.g. random or pseudo random noise. The way to obtain the FRF is not important. However, it is important to be able to control the level of excitation. If the level of input can not be controlled, it is not possible to conclude anything regarding the range of a systems linear and nonlinear regime.

6.4 Extension to General Systems

Recalling from the introduction that nonlinear systems are highly individualistic, it is important to note that the results presented in this paper are only valid for the tested systems. It is only possible to speculate on the performance of the methods applied to other types of systems, and more extensive tests must be made to make more general conclusions. Both detection methods are based on FRF distortions. In the simple system tested, even weak nonlinearities influenced the FRF. In a larger system, weak nonlinearities might be present in sub systems that will not influence the global system's FRF enough to be detected. Therefore, for detection in larger and more complex systems it might be necessary to excite and evaluate small sub systems to detect localized nonlinearities.

7 Conclusions

Two methods for experimental detection of structural nonlinearity were tested, and a nonlinearity index was suggested. Both method where tested on both simulated and experimental data. In the simulation study it was shown that both methods were able to detect three types of nonlinearities, smooth and nonsmooth stiffness, and smooth damping nonlinearity. Both methods were least sensitive to damping nonlinearities. For all three types of nonlinearities it was observed that the homogeneity methods was the most sensitive of the two methods. In the experimental study only the two types of stiffness nonlinearities were tested. As for the simulation study, it was observed that the homogeneity method had a greater sensitivity than the Hilbert transform based method.

Acknowledgements

This work was supported by the Otto Mønsted Foundation and by Brüel & Kjær Sound & Vibration Measurement.

References

[1] G. Kerschen, K. Worden, A. F. Vakakis, and J. C. Golinval. Past, present and future of nonlinear system identification in structural dynamics. *Mechanical Systems and Signal Processing*, 20:505–592, 2005.

[2] J. M. Nichols, P. Marzocca, and A. Milanese. On the use of the auto-bispectral density for detecting quadratic nonlinearities in structural systems. *Journal of Sound and Vibration*, 312:726–735, 2008.

[3] J. M. Nichols, P. Marzocca, and A. Milanese. Nonlinearity detection in multiple-degree-of-freedom systems using the auto-bespectral density. *Proceedings of SPIE, 6935:39650N1-8,2008*, 6935, 2008.

[4] Y. H. Chong and M. Imregun. Use of reciprocal vectors for nonlinearity detection. *Archive of Applied Mechanics 70*, 70:453–462, 2000.

[5] I. Trendafilova, M. P. Cartmell, and W. Ostachowicz. Vibration-based damage detection in an aircraft wing scaled model using principal component analysis and pattern recognition. *Journal of Sound and Vibration*, 313:560–566, 2008.

[6] M. Simon and G. R. Tomlinson. Use of the Hilbert transform in modal analysis of linear and non-linear structures. *Journal of Sound and Vibration*, 96:421–436, 1984.

[7] G. R. Tomlinson. Developments in the use of the Hilbert transform for detecting and quantifying non-linearity associated with frequency response functions. *Mechanical Systems and Signal Processing*, 1:151–171, 1987.

[8] G. Kerschen, M. Peeters, and A.F. Vakakis J.C. Golinval. Nonlinear normal modes part 1: An attempt to demystify them. *Mechanical Systems and Signal Processing*, 23:170–194, 2009.

[9] M. Peeters, R. Viguie, G. Serandour G. Kerschen, and J.C. Golinval. Nonlinear normal modes part 2: Practical computation using numerical continuation techniques. *Mechanical Systems and Signal Processing*, 23:195–216, 2009.